The Contribution of Mesoscale Convective Complexes to Rainfall across Subtropical South America

JOSHUA D. DURKEE

*Meteorology Program, Department of Geography and Geology, Western Kentucky University,
Bowling Green, Kentucky*

THOMAS L. MOTE AND J. MARSHALL SHEPHERD

Climate Research Laboratory, Department of Geography, University of Georgia, Athens, Georgia

ABSTRACT

This study uses a database consisting of 330 austral warm-season (October–May) mesoscale convective complexes (MCCs) during 1998–2007 to determine the contribution of MCCs to rainfall across subtropical South America (SSA). A unique precipitation analysis is conducted using Tropical Rainfall Measuring Mission (TRMM) 3B42 version 6 data. The average MCC produces 15.7 mm of rainfall across 381 000 km^2, with a volume of 7.0 km^3. MCCs in SSA have the largest precipitation areas compared to North American and African systems. MCCs accounted for 15%–21% of the total rainfall across portions of northern Argentina and Paraguay during 1998–2007. However, MCCs account for larger fractions of the total precipitation when analyzed on monthly and warm-season time scales. Widespread MCC rainfall contributions of 11%–20% were observed in all months. MCCs accounted for 20%–30% of the total rainfall between November and February, and 30%–50% in December, primarily across northern Argentina and Paraguay. MCCs also produced 25%–66% of the total rainfall across portions of west-central Argentina. Similar MCC rainfall contributions were observed during warm seasons. An MCC impact factor (MIF) was developed to determine the overall impact of MCC rainfall on warm-season precipitation anomalies. Results show that the greatest impacts on precipitation anomalies from MCC rainfall were located near the center of the La Plata basin. This study demonstrates that MCCs in SSA produce widespread precipitation that contributes substantially to the total rainfall across the region.

1. Introduction

Mesoscale convective complexes (MCCs) are a frequently occurring subclass of mesoscale convective systems (MCSs) that are widely observed around the globe. These large, long-lasting organized systems are comprised of an ensemble of thunderstorms that together, often yield intense rain rates within contiguously sizeable precipitation areas and can greatly influence the hydroclimate of a region. One such region that has been shown to have a high frequency and concentration of MCCs during the austral warm season (defined here as October–May) is the La Plata basin (Fig. 1). The

La Plata basin is the fifth-largest drainage basin in the world (3.2×10^6 km^2), located east of the Andes Mountains primarily between 20° and 40°S [also referred to herein as subtropical South America (SSA)], which drains the Paraná, Paraguay, and Uruguay River systems. Much of the economy of this densely populated region comes from agriculture and hydroelectric power demand, which is exceedingly reliant upon and vulnerable to heavy precipitation events (Mechoso et al. 2001).

Previous studies have shown that MCCs can account for large fractions of rainfall [e.g., up to 60% during the warm season in the central United States (Ashley et al. 2003; Fritsch et al. 1986), and 22% in Sahelian Africa (Laing et al. 1999)]. However, while several studies have examined the precipitation characteristics of MCSs in portions of South America, including MCCs, the current study is the first to examine the rainfall contributions from MCCs across all of SSA with a dataset that comprises nine
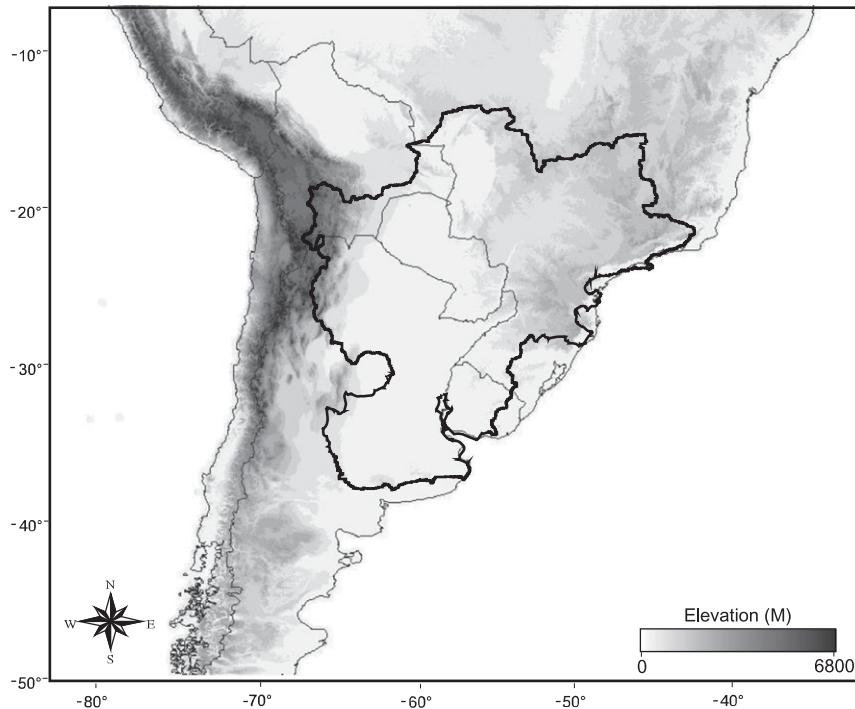
FIG. 1. Bold outline delineates the La Plata basin located in the subtropics of South America.

warm seasons. The goal of this work is to provide a better understanding of the role of convective rainfall in the precipitation climatology of SSA.

Warm-season precipitation in SSA largely exhibits a nocturnal maximum (Berbery and Collini 2000). Berbery and Barros (2002) identified a precipitation maximum over portions of Paraguay, northeastern Argentina, and southeastern Brazil throughout much of the warm season. Numerous studies have shown that the timing and location of precipitation maxima across SSA are modulated through the exchange tropical heat and moisture via the northerly low-level jet (Saulo et al. 2007; Vera et al. 2006; Silva and Berbery 2006; Liebmann et al. 2004; Zipser et al. 2006; Nieto Ferreira et al. 2003; Marengo et al. 2004; Berbery and Collini 2000; Laing and Fritsch 2000; Nicolini and Saulo 2000). Many of these studies have demonstrated that the low-level jet plays a vital role in the development and maintenance of predominantly nocturnal MCSs within the subtropical region. Zipser et al. (2006) found these subtropical South American MCSs are among the world's most intense thunderstorms.

The foundational study of South American MCCs from Velasco and Fritsch (1987) provided the initial evidence of MCC activity in SSA, but did not assess MCC rainfall. Viana (2006) examined MCCs in the southern state of Rio Grande do Sul, Brazil, and found that these events contributed an average of 63% of the total rainfall

between October and December in 2003. Mota (2003) examined large MCSs from December 1997 to November 2000 and found that these events contributed up to half of the total rainfall across portions of SSA. Salio and Nicolini (2007) suggested that MCSs are the dominant contributor to precipitation totals across the region. Although many of these studies provide initial evidence of these large thunderstorm complexes producing considerable proportions of the total rainfall across SSA, a climatological understanding of rainfall contributions from these systems has remained unknown.

Durkee and Mote (2009) described the climatological characteristics of 330 warm-season MCCs across SSA for 1998–2007. Their results established that the region with the greatest frequency and highest concentration of MCCs coincides well with the location of the precipitation maximum described by Berbery and Collini (2000). Durkee and Mote (2009) also showed that these systems are predominantly nocturnal, which also matches well with the nighttime precipitation maximum highlighted by Berbery and Barros (2002). Consequently, one may ask if the precipitation patterns found throughout the warm season across SSA may be ascribed, in part, to relatively frequent and concentrated MCC activity near the center of the La Plata basin.

The findings from Durkee and Mote (2009) showed that, on average, these austral systems are statistically significantly larger and longer lived than MCCs in the
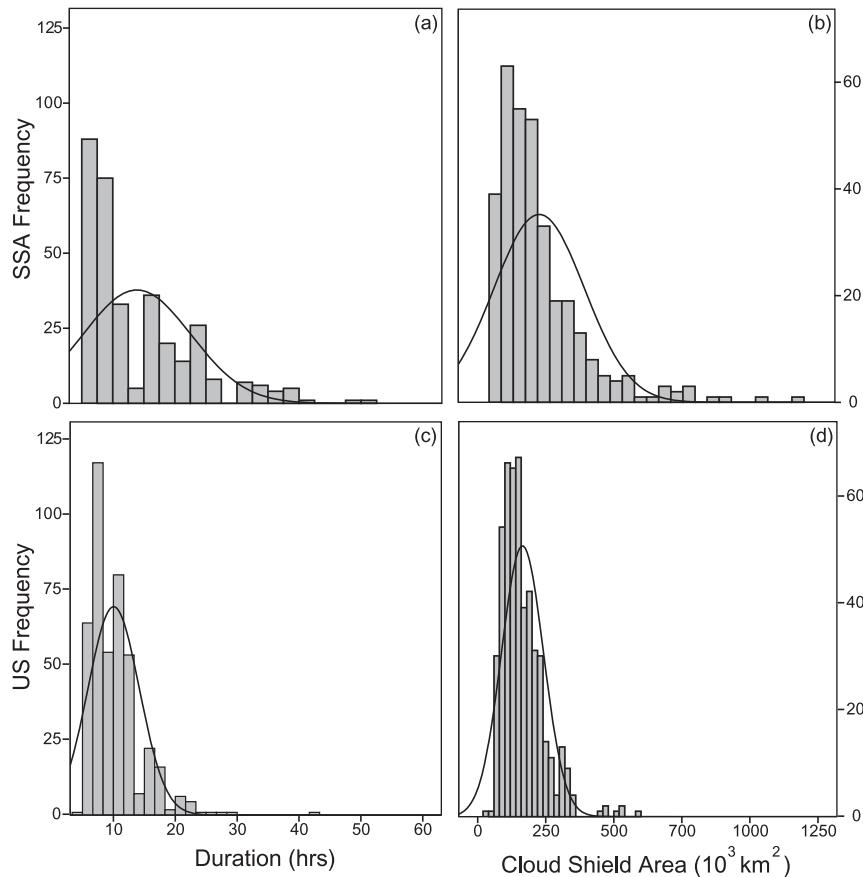
FIG. 2. Histograms of duration for MCCs in (a) SSA and (b) the United States, and histograms of MCC cloud shield areas in (c) SSA and (d) the United States.

United States. They showed that MCCs in SSA reach an average maximum size of 256 500 km² and last 14 h (compared to 164 600 km² and 10 h in the United States; $p = 0.01$). Histograms from the data provided by Durkee and Mote (2009) show that numerous smaller, shorter-lived South American systems are similar in size and duration to the larger, longer-lasting events in the United States (Fig. 2). Tollerud et al. (1987) and Ashley et al. (2003) found that larger, longer-lived MCCs commonly produce the greatest precipitation amounts. These results raise the question regarding MCC precipitation across SSA: do the physical characteristics described in Durkee and Mote (2009) suggest that relative to the United States, MCCs in SSA contribute more to the total warm-season rainfall?

In support of the findings and suggestions of previous work described above, the findings from Durkee and Mote (2009) provide strong evidence that the precipitation variability across SSA is connected with MCC rainfall. The initial work of Viana (2006) and Mota (2003) further supports this hypothesis. However, there are no available studies that provide a long-term exami-

nation of MCC rainfall contributions across SSA. Therefore, the overarching goal of this study is to determine the contribution of MCCs to warm-season rainfall across SSA for 1998–2007.

2. Data

To determine precipitation characteristics of warm-season MCCs across SSA, this study utilized the dataset assembled in the Durkee and Mote (2009) study, which contains 330 MCCs. These systems were identified and tracked from full-disc *Geostationary Operational Environmental Satellite (GOES)-8* and *GOES-12* 4-km infrared (IR) satellite data, which were provided by the National Oceanic Atmospheric Administration (NOAA) Comprehensive Large Array-Data Stewardship System (CLASS; data available online at http://www.class. ncdc.noaa.gov). The nominal times for the satellite images were 0245, 0545, 0845, 1145, 1445, 1745, 2045, and 2345 UTC. There were occasional instances when nominal image times were missing, but they were available during other times (e.g., 0915 UTC).

Analyzing precipitation characteristics for specified thunderstorm events across South America presents a number of challenges. The primary difficulty is finding an available dataset that contains a consistently quality-controlled long-term record with a sufficient temporal sampling resolution and network density to capture the mesoscale precipitation variability within all 330 MCCs. For example, the Global Precipitation Climatology Centre (GPCC) provides global land-based accumulated rainfall data for the period of record, but only at monthly time scales with 1° resolution (information online at http://www.dwd.de). The World Climate Research Programme's (WCRP's) Global Precipitation Climatology Project (GPCP) provides rainfall data for the period of record from merged passive microwave and land-based estimators, but only at daily time scales with 1° resolution (available at ftp://rsd. gsfc.nasa.gov/pub/1dd/). Furthermore, while Visible and Infrared (VISIR) approaches often provide relatively greater spatial and temporal resolution, the accuracy of these approaches primarily suffers from using cloud attributes as a proxy for estimating precipitation. Therefore, the nominal approach for quantifying precipitation for a relatively large subset of MCCs over the entire SSA region is to utilize a high-quality data source derived from blended precipitation sampling methods [e.g., Tropical Rainfall Measuring Mission (TRMM)].

One of the objectives of TRMM during its inception in December 1997 was to provide relatively high temporal and spatial rainfall data, particularly for poorly sampled regions (Kummerow et al. 2000). This study uses TRMM Multisatellite Precipitation Analysis (TMPA) 3B42 version 6, which provides global 3-hourly precipitation rate estimates with latitudinal coverage between 50°N and 50°S (0.25° grid) from 1998 January to the present (information at http://disc.sci.gsfc.nasa.gov/data/ datapool/TRMM). The 3B42 product is derived from an amalgamation of passive microwave estimates from the onboard TRMM Microwave Imager (TMI), Special Sensor Microwave Imager (SSM/I), Advanced Microwave Sounding Unit (AMSU), Advanced Microwave Scanning Radiometer (AMSR), and calibrated IR estimates from geostationary platforms [consult Huffman et al. (2007) and Huffman and Bolvin (2007) for explicit details on the TMPA algorithm and 3B42 processing].

Huffman and Bolvin (2007) discuss two concerns with the 3B42 dataset. First, the orbital altitude of the TRMM platform was increased from 350 to 401.5 km in August 2001. Because of the success of TRMM, the boost was carried out for fuel reduction to increase the longevity of the project. The advantage was an increase in the latitudinal coverage from 40°N–40°S to 50°N–

50°S. However, changes in the footprint and minimum detectable precipitation rates occurred. Although version 6 of the dataset attempts to account for these discrepancies, some differences in the minimum detectable rain rates can still be found. Second, the latitude bands of 40°–50°S only contain passive microwave estimates between 1 January 1998 and 6 February 2000. This is particularly problematic given the limited availability of passive microwave data during this time (i.e., there were a few passes a day that systematically missed precipitation). Therefore, all MCCs with cloud shield areas beyond 40°S were flagged for potential precipitation errors during this time.

Another important consideration is the robustness of passive microwave rainfall estimates of mesoscale phenomena over land areas. First, the use of passive microwave data to distinguish rain over land is ambiguous using low-frequency (i.e., <22 GHz) absorption methods because of the similar emissivities of land and rainfall. Therefore, scattering techniques using high-frequency channels (i.e., 85 GHz) are used to associate the concentration of ice particles with precipitation. According to Ebert et al. (2007), scattering techniques are particularly useful in estimating precipitation from midlatitude convective systems. Furthermore, Ebert et al. (2007) provide a land-based comparative analysis of TMPA data against relatively dense rain gauge networks across the United States, Australia, and northwest Europe. Results from their study showed that the accuracy of satellite-derived rainfall totals is greatest during the warm season and increases toward the lower latitudes, particularly with respect to deep convective precipitation regimes. Ebert et al. (2007) also found that in the United States, TMPA rainfall estimates were near that of radar estimates for daily precipitation bias and frequency. Sapiano and Arkin (2009) showed that TMPA exhibited little bias in warm-season convective precipitation estimates over the Great Plains in the United States, when compared to rain gauge estimates. Second, 3B42 data have been suggested as suitable metrics for long-lived meso-α systems,[1] particularly when analyzed in a climatological framework. Considering the relative minimum bias in TMPA warm-season rainfall estimates, and that this study focuses on warm-season MCCs over the subtropical landmass of South America for the period of 1998–2007, 3B42 data are considered a unique, viable source for quantifying MCC rainfall (G. J. Huffman 2007, personal communication; Huffman et al. 2007).

---

[1] Meso-α scale has length scales of 250–2500 km and a duration of ≥6 h (Orlanski 1975).

TABLE 1. Mesoscale convective complex definition based on analyses of enhanced IR satellite imagery. The MCC definition was originally developed by Maddox (1980).

MCC definition	
Criterion	Physical characteristics
Size	An interior cold-cloud region with a temperature of $-52°C$ must have an area 50 000 km^2
Initiation	Size definition is first satisfied
Duration	Size definition must be met for a period of ≥ 6 h
Maximum extent	Contiguous cold-cloud shield (IR temperature $-52°C$) reaches maximum size
Shape	Eccentricity (minor axis/major axis) is 0.7 at the time of maximum extent
Terminate	Size definition is no longer satisfied

3. Methodology

The MCC identification and tracking method outlined in Durkee and Mote (2009) included a hybrid automated–manual observation approach that conformed to specific MCC criteria (Table 1). First, an automated routine identified various characteristics (see below) of cloud shields that met MCC size and temperature criteria. Next, the cloud shields were manually tracked from a sequence of satellite images in order to identify individual MCC events. MCC evolution, including splitting and merging systems, were delineated following Machado et al. (1998). From that work, there were two outputs necessary for this study. The first is a list of events where each observed cloud shield was tagged with a unique identifier based on the event number for a given year, Julian day, and time of occurrence. These cloud shields included data on horizontal area, eccentricity, and centroid coordinates. The second output contained the longitude–latitude coordinates that make up the outer perimeter of the continuous cold-cloud shield. Additional details concerning these methods are provided by Durkee and Mote (2009).

The first step toward quantifying MCC precipitation was to use data from the output files to determine the aerial swath of each event's storm track. For this study, MCC precipitation was assumed to fall solely within this swath. It is important to note that some previous studies examined MCC precipitation from a cloud-top threshold of $-32°C$ (e.g., Viana 2006; Ashley et al. 2003). However, the colder cloud-top threshold of $-52°C$ was used in this study because MCC precipitation areas are mostly confined to areas beneath these colder cloud shields (McAnelly and Cotton 1986, 1989), and it has been widely used in other MCC studies (e.g., Augustine and Howard 1988; Anderson and Arritt 1998; Laing et al. 1999; Anderson and Arritt 2001).
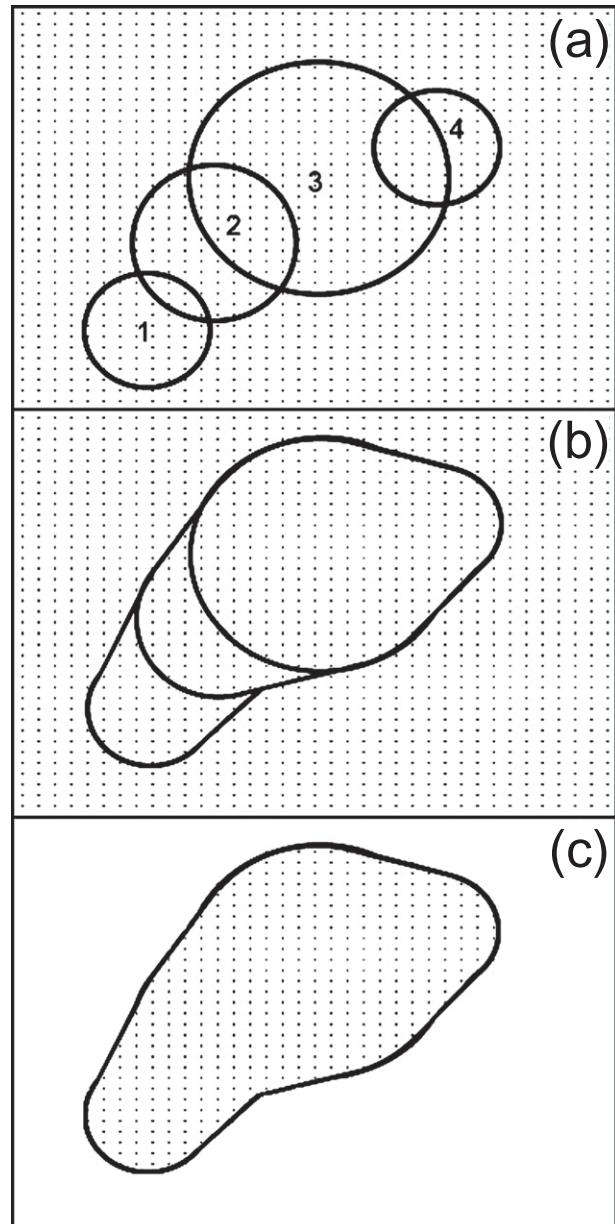
FIG. 3. Schematic diagram illustrating (a) cloud shields of an MCC overlaid onto a TRMM 3B42 precipitation grid, (b) the convex hull calculation to determine the area within the MCC storm track, and (c) the final convex hull for the entire MCC duration, retaining only precipitation values within the storm-track area.

To demarcate the storm-track aerial coverage, a convex hull was calculated throughout each event's life cycle (see Barber and Huhdanpaa 1996) and overlaid onto 3B42 precipitation grids. For example, Fig. 3 shows a hypothetical MCC observed across a sequence of four satellite images. For the series of cloud shields, a convex hull is computed to determine the aerial storm-track

Observed MCC lifecycle (IR image times)
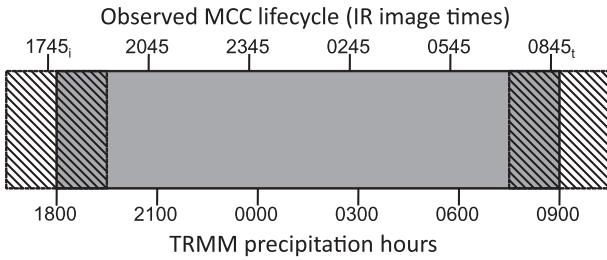
FIG. 4. Schematic representation of the precipitation summation for a hypothetical event. Hatched boxes are centered on the synoptic times closest to the event's initiation (subscript "i") and termination (subscript "t") stages. Precipitation values inside the hatched boxes are assigned a weight of 0.5. Precipitation values inside the solid gray box are assigned a weight of 1.0. Accumulated precipitation is equal to the sum of all weighted observations.

swath for the first and second observations, followed by the second and third, and third and fourth. Precipitation values within the convex hull were tracked and recorded in sequence throughout the duration of each event. The end product is a mask that represents the location of the total surface area and accumulated precipitation beneath an MCC during its life cycle.

Figure 4 shows a schematic diagram of the precipitation summation scheme of a hypothetical event. It is also important to note that 3-hourly TRMM 3B42 precipitation data represent instantaneous values centered on synoptic times (i.e., 0000, 0300, 0600, 0900, 1200, 1500,

1800, and 2100 UTC). Given the nominal times of the imagery, a weighting factor of 0.5 was applied to all of the precipitation values within 1.5 h on either side of the system's initiation and termination (1745 and 0845 UTC in Fig. 4, respectively). The solid gray box signifies precipitation values weighted to unity. Accumulated rainfall is simply the average of all of the weighted rain rates multiplied by the number of hours in the event.

The output contained aerially averaged precipitation totals and total precipitation areas associated with each of the 330 events. The accumulated rainfall was also tabulated for each grid point within the convex hull for each event, and summed into both monthly and warmseason totals. An output file was created, where each scene contained the outline of the convex hull mask and accumulated precipitation was produced as a verification check of this process (Fig. 5). Last, monthly and seasonal summations of 3B42 data were determined for all of the precipitation (i.e., from MCCs and all other rainfall events). The contribution of MCC rainfall is expressed as the ratio of MCC precipitation to the total rainfall at each grid point. A summary of the entire process is illustrated in Fig. 6.

4. Results

MCCs between 1 January 1998 and 6 February 2000 were screened for cloud shield areas south of 40°S to

09 025   01/11/2007 (011) 05:45UTC - 01/11/2007 (011) 11:45UTC
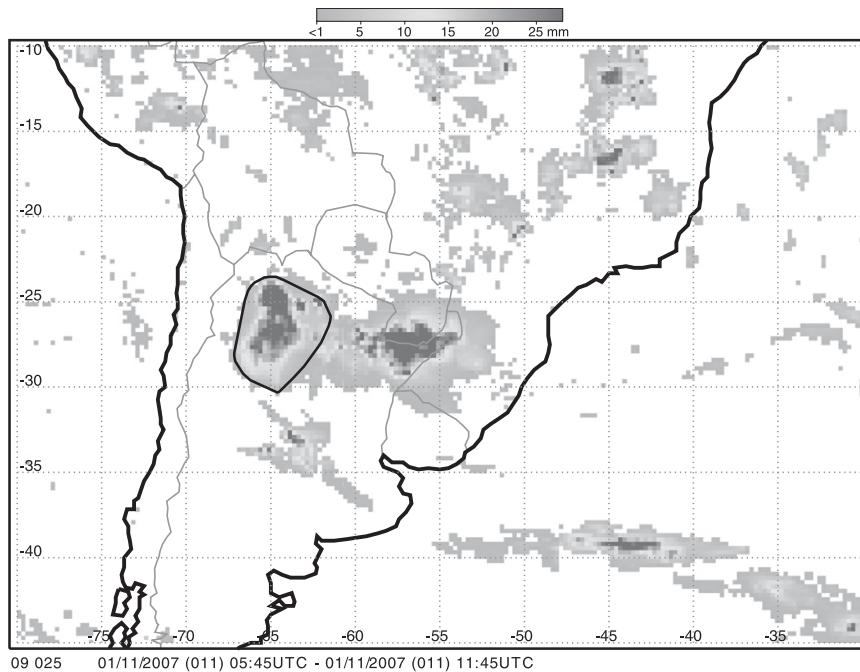
FIG. 5. Sample output illustrating the outline of the area (i.e., convex hull) of an MCC storm track overlaid with accumulated 3B42 TRMM precipitation.
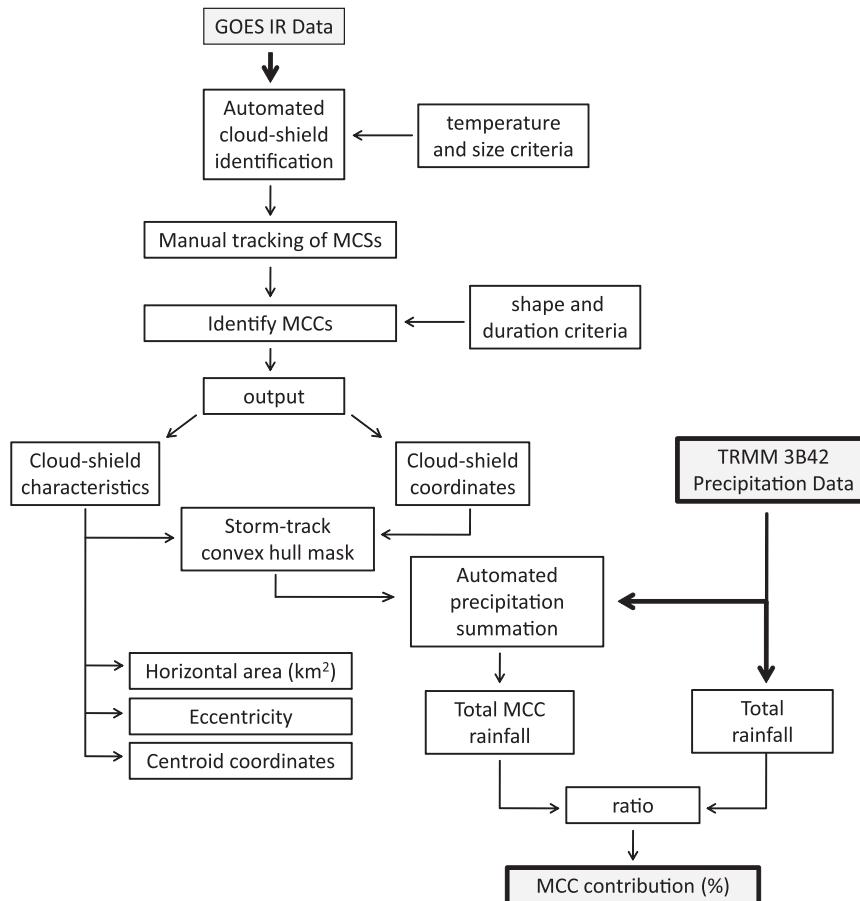
FIG. 6. Flow diagram demonstrating the MCC identification and tracking, and precipitation schemes.

assess for potential precipitation discrepancies (see section 2). Four events had distinct discontinuities in precipitation data between 40° and 50°S. The data in question only accounted for less than 2% of the total precipitation observed for these events. Therefore, precipitation south of 40°S for these events was removed from further analysis.

a. Period of record

The average MCC in SSA produces 15.7 mm of rainfall over an area of 381 000 km^2, with a volume of 7.0 km^3. A comparison of mean precipitation characteristics for MCCs in South America, Africa (Laing et al. 1999), and the United States (McAnelly and Cotton 1989) is shown in Table 2. MCC precipitation depths and volumes found in this study fall between African and U.S. systems, but produce the largest precipitation areas. These larger precipitation areas are accounted for by larger MCCs in South America (cf. Durkee and Mote 2009; McAnelly and Cotton 1989; Laing and Fritsch 1993). However, the precipitation characteristics described by McAnelly and Cotton (1989) might be con-

servative given they only considered late warm-season events. Ashley et al. (2003) showed that late-season MCCs in the United States are commonly much smaller, shorter-lived systems. Another critical factor among these differences may likely stem from data sources and approaches used in each study. For example, McAnelly and Cotton (1989) used an hourly surface rain gauge network and Laing et al. (1999) used an SSM/I-derived precipitation product. Both of these sources of precipitation data are included in TMPA, which is used in the current study.

TABLE 2. Comparison of MCC precipitation characteristics between South America (SA), Africa (AF) (Laing et al. 1999), and the United States (US; McAnelly and Cotton 1989).

Mean precipitation characteristics				
MCCs		Depth (mm)	Area (km^2)	Volume (km^3)
SA	330	15.7	381 000	7.0
AF	41	34.0	285 000	11.9
US	122	10.8	320 000	3.5
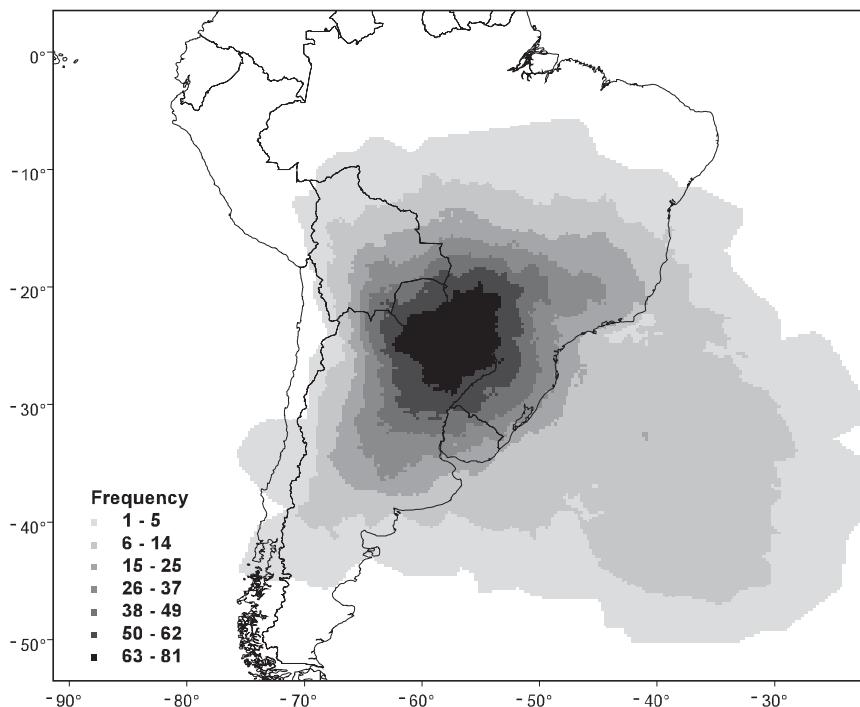
FIG. 7. MCC frequency during the warm season (October–May) for 1998–2007 (N = 330) determined by the number of times a grid point was located inside an MCC storm track.

A spatial examination of the 330 MCC storm tracks shows the greatest MCC frequencies over Paraguay, northern Argentina, and southern Brazil (Fig. 7). The geographic distribution of the fractional contribution of MCC rainfall revealed a similar pattern (Fig. 8). Specifically, 15%–21% of the total precipitation in northern Argentina and portions of Paraguay was accounted for by MCCs. These values appear low compared to the results of Mota (2003) and Viana (2006) (40%–50% and 63%, respectively). These differences are likely attributed to the period of record and the methods used in their studies. For example, Mota (2003) used a precipitation feature algorithm (see Nesbitt et al. 2000) to identify 3 yr of MCSs based on criteria that are different from that Table 1, which likely included a considerable sample of events smaller than MCCs. Viana (2006) used 31 rain gauges to determine MCC rainfall contributions. The results found by Viana (2006) may also be reflective of only examining a 3-month record (October–December 2003). Furthermore, Viana (2006) used a warmer cloud-top threshold of −32°C, which accounts for the potentially larger precipitation areas and totals.

b. Monthly analysis

MCCs contributed 11%–20% of the total rainfall across much of SSA in all months (Fig. 9). Paraguay and northern Argentina consistently received the largest fraction of total precipitation from MCCs. Between November and February, much of Paraguay and northern Argentina received 20%–30% of the total precipitation from MCCs. The maximum contributions of MCCs to rainfall were found across northern Argentina and portions of Paraguay and southeastern Brazil during December (30%–50%).

At times, portions of west-central Argentina also received considerable percentages of MCC rainfall. The area largely within the provinces of Mendoza, Neuquén, and La Pampa received 25%–44% of the total precipitation from MCCs during October. MCCs contributed 30%–66% and 30%–40% of the precipitation to the same area during November and May, respectively. The findings from Durkee and Mote (2009) and Velasco and Fritsch (1987) showed that MCCs are infrequent to this particular area (see Fig. 7). It is likely that areas infrequent to MCCs tend to experience greater fractional rainfall contributions from MCCs when they do occur.

This study shows that the fraction of precipitation resulting from MCCs is larger for much of SSA compared to the United States. Ashley et al. (2003) found that MCCs contributed 10%–20% of the monthly rainfall across the central United States, with maximum values of 28%. Results from this study indicate that monthly precipitation patterns across SSA are influenced more from MCCs.
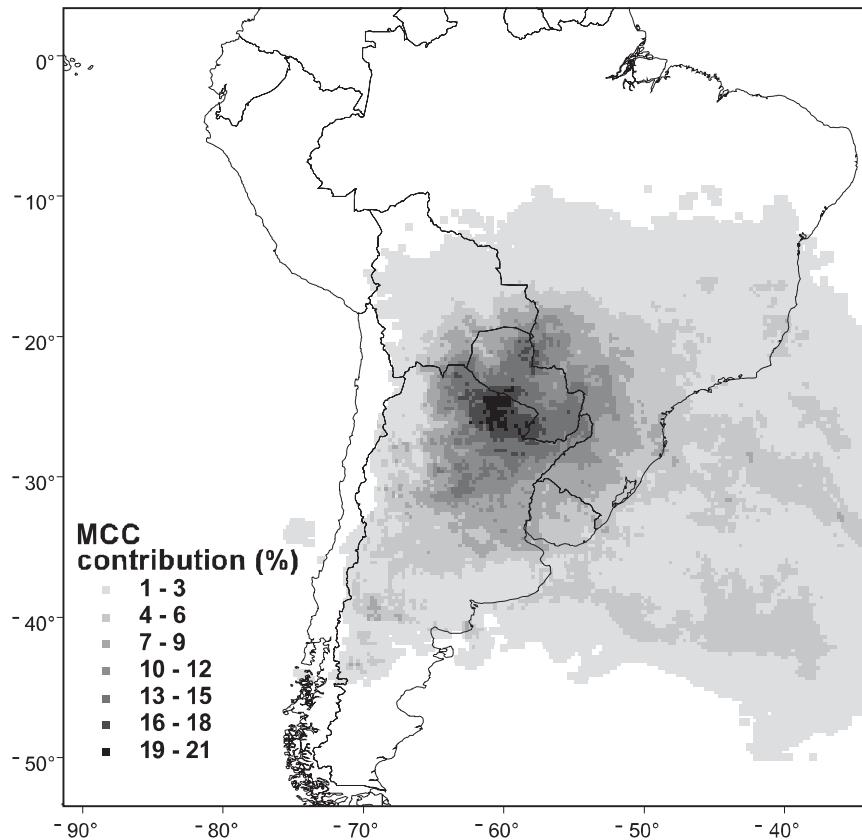
FIG. 8. Distribution of the percent of warm-season MCC rainfall during 1998–2007.

c. Warm-season analysis

An examination of the interannual variability in MCC precipitation contribution basis shows considerable spatial variability (Fig. 10). During each of the nine warm seasons, much of Paraguay and its neighboring border areas experienced the most MCC activity. As expected, the majority of the largest fractions of total rainfall resulting from MCCs were found in these areas. MCCs contributed 11%–20% of the warm-season rainfall across much of SSA, but it was not uncommon to find 40%–50% across portions of northern Argentina, Paraguay, and southern Brazil during most warm seasons.

It is clear that MCCs contribute substantially to warm-season precipitation across SSA. Some studies have suggested that MCC rainfall plays a potentially important role in regional rainfall budgets (e.g., Fritsch et al. 1986; Anderson and Arritt 1998; Ashley et al. 2003). However, no such relationships have been shown for SSA. One way to assess the impact of MCC precipitation beyond rainfall contributions is to examine warm-season precipitation anomalies with and without MCC rainfall. For this study, warm-season precipitation anomaly maps were constructed using mean TRMM 3B42 data for January 1998–December 2007 as a baseline for comparison. Precipitation anomalies were determined as the difference between observed and mean values. Warm-season precipitation anomalies for the period of record are shown in Figs. 11 and 12.

The warm seasons of 1998/99, 2000/01, and 2002/03 had similar MCC frequencies with maximum fractional contributions of rainfall totaling 33% (see Fig. 10). Each of these warm seasons also experienced three different precipitation anomaly conditions. The greatest fractional contributions of MCC rainfall were located in areas that were close to average warm-seasonal rainfall. However, above-average precipitation extended from Argentina into southeastern Brazil in 2002/03, the same area where MCCs contributed the least rainfall. The 2000–01 warm season experienced mostly average and some above-average rainfall, yet MCCs contributed the least amount of the total rainfall during this time. These findings raise the following question: how does the spatial variability in warm-season precipitation anomalies for the period of record change in the absence of MCC rainfall? The answer to this question provides a clearer understanding of
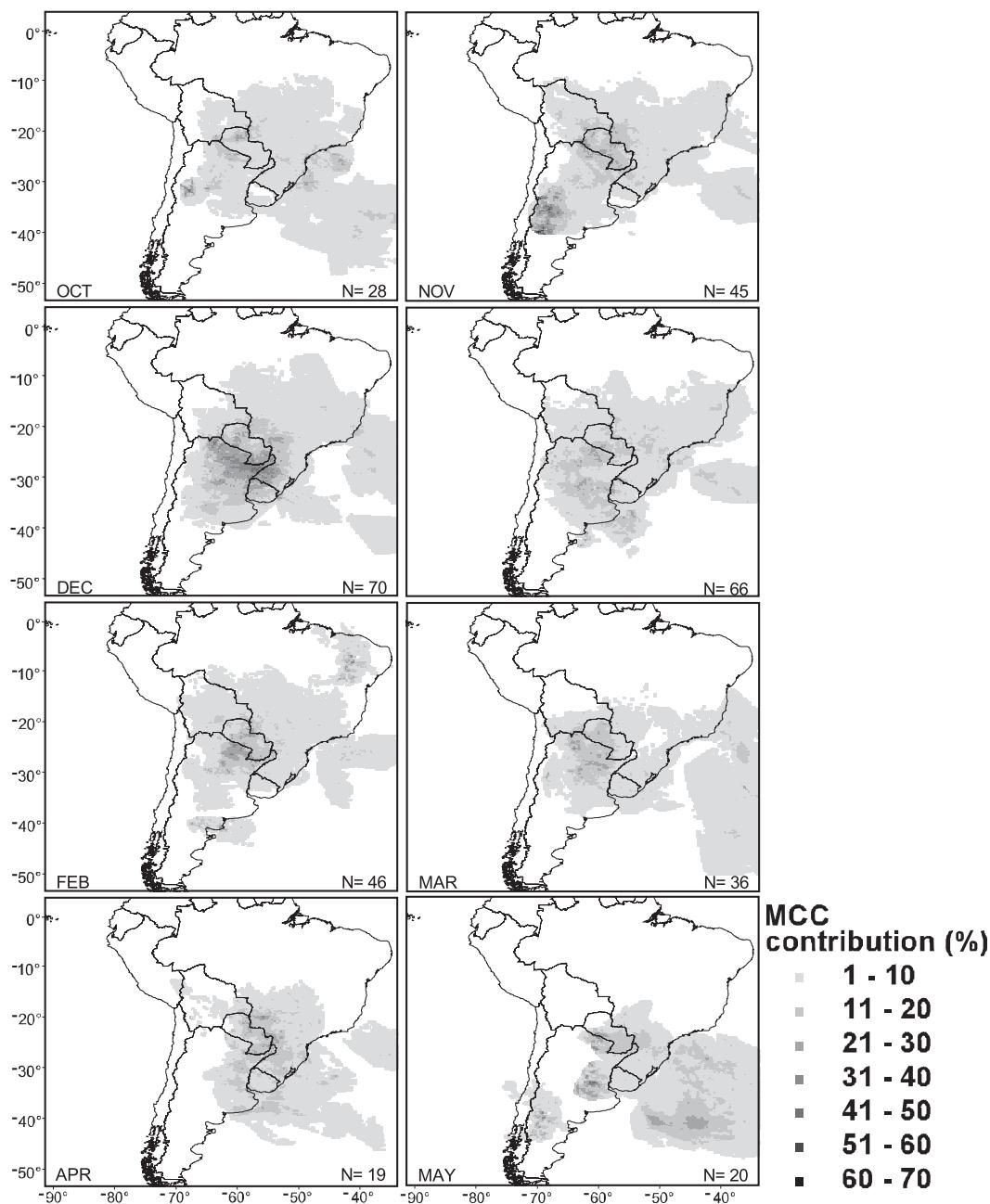
FIG. 9. Same as in Fig. 7, but by month.

the influence of MCCs by identifying only those areas with the greatest differences in precipitation anomalies resulting from MCC rainfall.

Visual assessments of such differences were difficult to discern from a 0.25° grid resolution, even in some areas (e.g., northern Argentina) where MCC fractions were large. To determine the extent and magnitude of the effect of MCC rainfall on warm-season precipitation anomalies, a MCC impact factor (MIF) was developed.

The MIF simply shows the contribution of MCCs to seasonal rainfall anomalies given by MIF $= (R_y - \overline{R}) - R_{\mathrm{mcc}}/2\sigma_{\mathrm{RA}}$, where R_y is the total rainfall for a given year, $\overline{R}$ is the climatological mean rainfall, R_{mcc} is the total MCC rainfall, and σ_{RA} is the standard deviation of the rainfall anomaly. Only grid points that contained differences between the anomaly value and MCC rainfall $(\Delta\sigma_i) \geq 0.5$ standard deviations were considered. The MIF ranking scale ranges from 1 to 6 at 0.5 standard
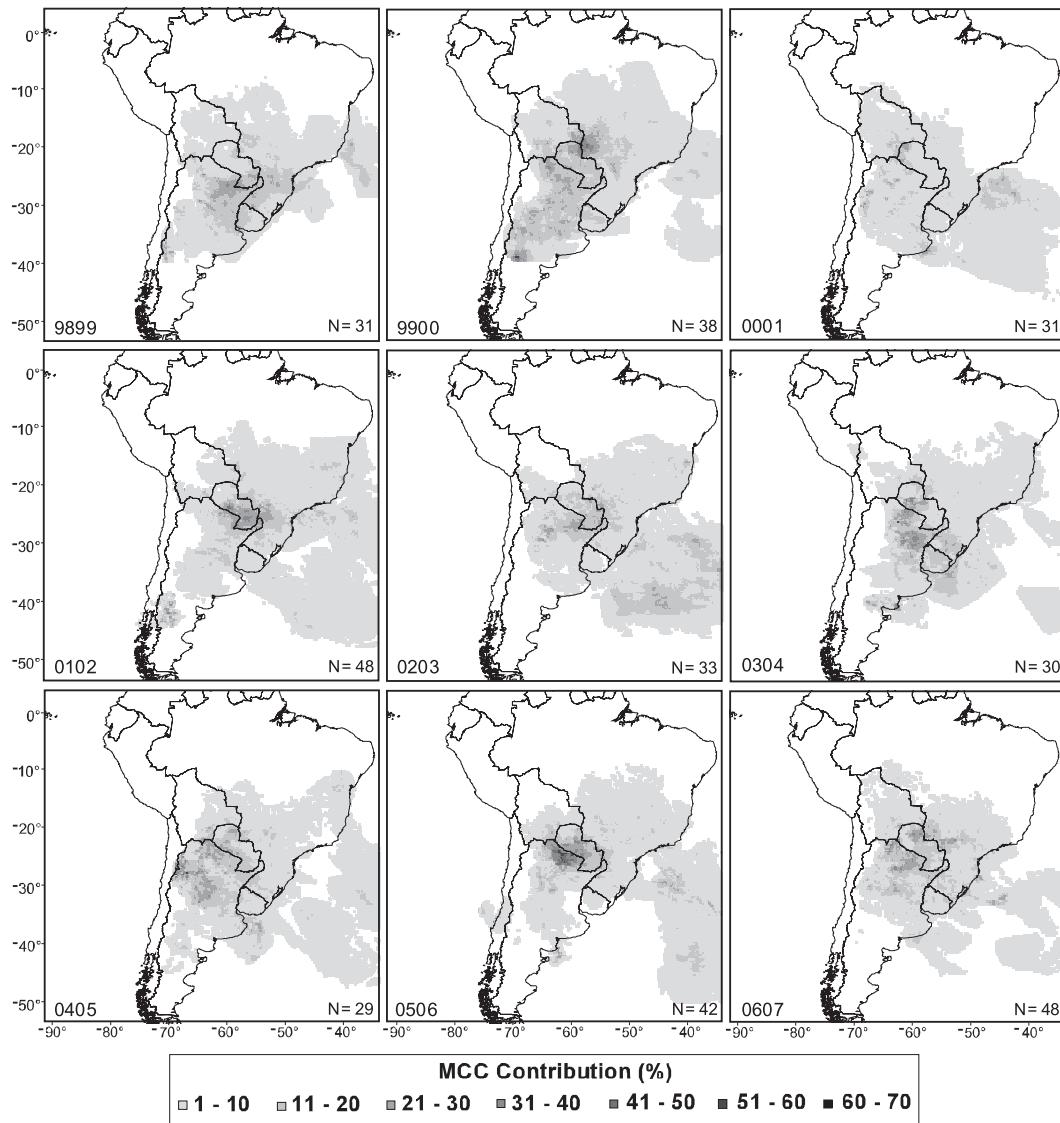
FIG. 10. Same as in Fig. 7, but by warm season.

deviation intervals. For example, MIF-1 indicates a 0.5–1.0 standard deviation change in the precipitation anomaly, whereas MIF-6 indicates a ≥3.0 standard deviation change. The locations of the greatest impacts from MCC rainfall during each warm season are illustrated in Fig. 13.

The analysis revealed that the impact of MCC precipitation on anomalous precipitation patterns varies considerably in extent and magnitude. MIF-1 was found in all warm seasons. The 2000/01 warm season was unique in that only MIF-1 was observed. However, many MIF-1 locations were found in areas of below-average rainfall (particularly southern Brazil). The extent of the impact was greatest during 1999/2000 with MIF-1 as the dominant magnitude. Anomalously

dry conditions were collocated with zero impact across Uruguay, northeastern Argentina, and southeastern Brazil during 2005/06. Notice how MIF-4 and MIF-5 were collocated with near-average rainfall just to the northwest. Additionally, the extent of the overall impact is collocated well with the area of predominantly above-average rainfall during 2006/07. These results demonstrate that MCC rainfall has the capability to alter precipitation totals in ways that are potentially beneficial (drought deterrence) and/or detrimental (floods).

d. El Niño–Southern Oscillation

Numerous studies have demonstrated that El Niño–Southern Oscillation (ENSO) can modulate the synoptic
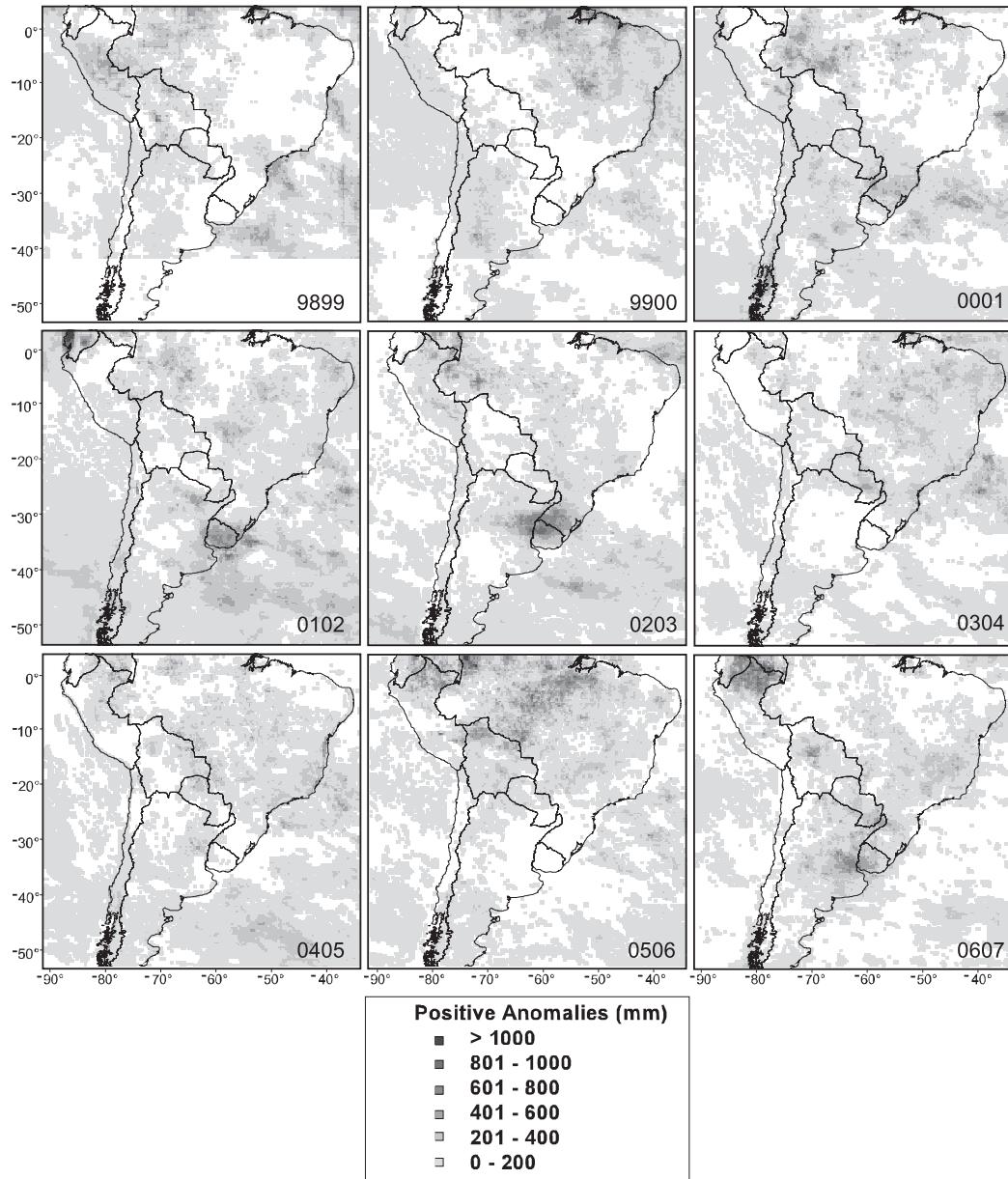
FIG. 11. Positive warm-season precipitation anomalies using 1998–2007 TRMM 3B42 as the baseline.

and mesoscale environments over South America, which in turn can influence convective activity and precipitation patterns across the tropical and subtropical regions (e.g., Curtis 2008; Silva and Ambrizzi 2006; Nieto Ferreira et al. 2003; Lau and Zhou 2003; Grimm et al. 2000, 1998; Ropelewski and Halpert 1989, 1987; Velasco and Frisch 1987). Specifically, Velasco and Fritsch (1987) found that the number of MCCs doubled during the 1982/83 El Niño event. However, Durkee and Mote (2009) showed no apparent relationship between MCC frequency and ENSO. Furthermore, additional analyses of ENSO and MCC cloud-top characteristics,

longevity, and the distribution of MCC rainfall and MIFs show no apparent relationship.

It is important to note that the study presented here is not suitable for statistical analyses of low-frequency variability of MCCs as it relates to ENSO (Carvalho et al. 2002); thus, these inferences should be tested with a considerably longer period of record. Perhaps the interannual and intraseasonal MCC variability found by Durkee and Mote (2009) and in the current study are reflective of other low-frequency modes of variability (e.g., South Atlantic convergence zone; Madden–Julian oscillation, Southern Hemisphere annular mode).
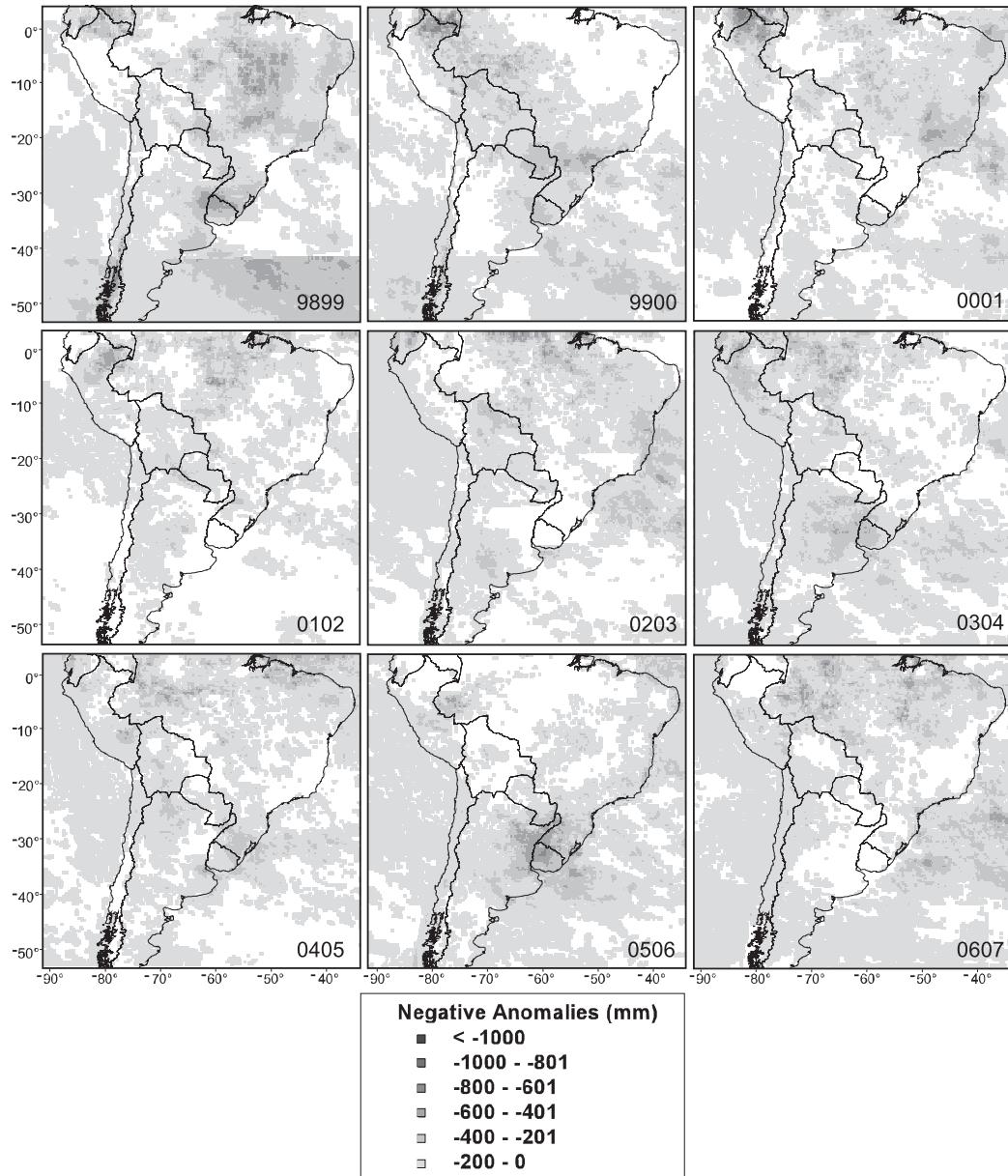
FIG. 12. Same as in Fig. 10, but for negative warm-season precipitation anomalies.

Together, these studies provide the opportunity to explore these possible relationships.

5. Summary and conclusions

This study provides a climatological description of the precipitation characteristics of 330 warm-season MCCs for 1998–2007. Results show MCCs contribute substantially to precipitation totals across SSA. It is clear from these examinations that a great degree of variability exists in contributions by MCCs to the total monthly and warm-season rainfall. This study also shows that MCCs

play a particularly important role in warm-season precipitation anomalies across SSA.

On average, MCCs in SSA distribute 15.7 mm of rainfall across 381 000 km^2, producing a volume of 7.0 km^3. South American systems have the largest precipitation areas compared to published studies for North America and Africa. Previous studies suggest that the physiographic arrangement of the Andes Mountains and abundant tropical supply of Amazonian heat and water vapor flux into the subtropical region are key factors in the development and maintenance of these large heavy precipitation events.
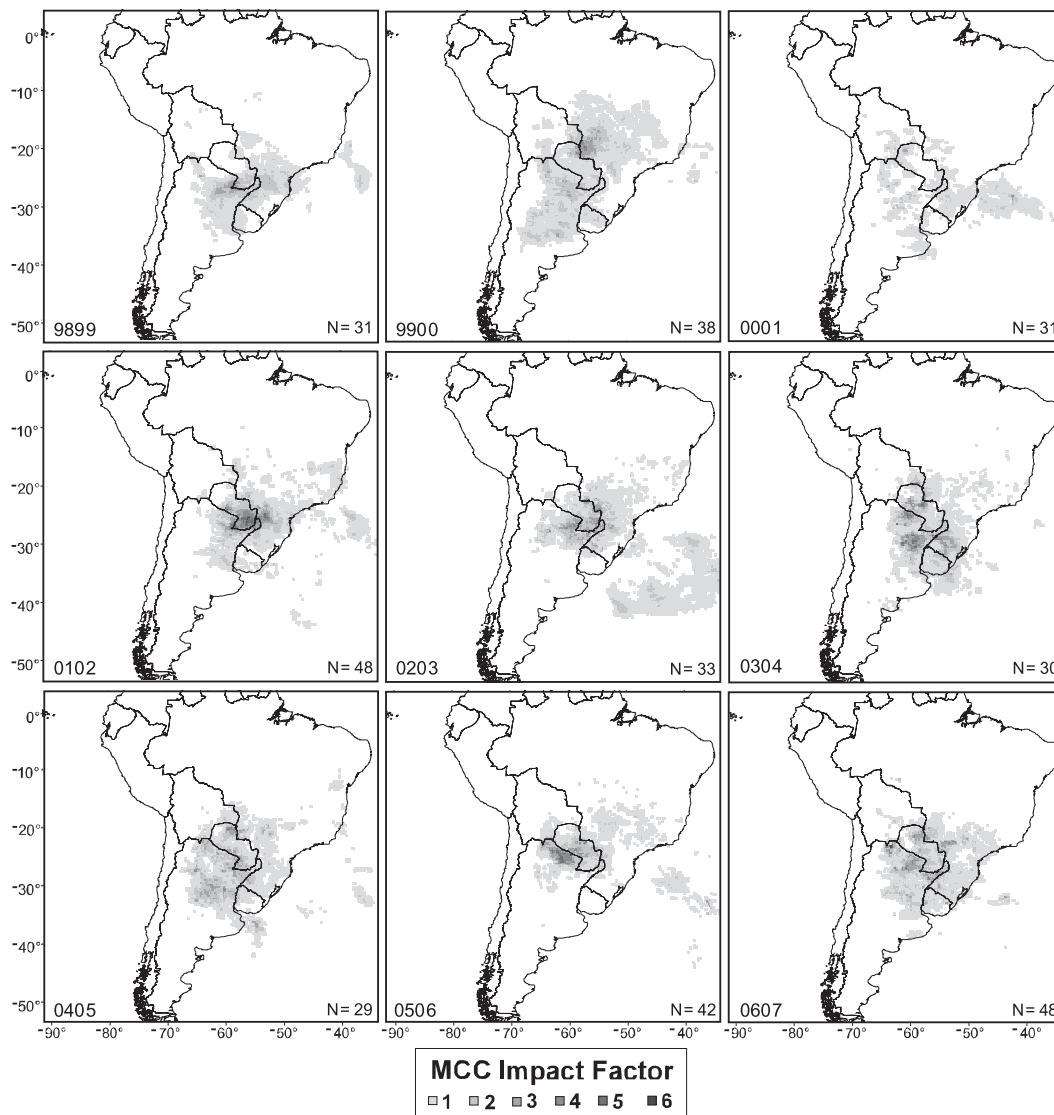
FIG. 13. MIFs are in 0.5 std dev unit intervals ranging from 1 to 6. Each grid point represents changes in the anomaly value by ≥ 0.5 std devs resulting from MCC precipitation ($\Delta\sigma_i$).

MCC storm-track frequencies and rainfall contributions were generally greatest over Paraguay and the surrounding areas of the neighboring countries. The extent of MCC rainfall was primarily east of the Andes between 10° and 45°S. For the period of record, portions of northern Argentina and Paraguay received 15%–21% of the total precipitation from MCCs. However, MCCs account for larger fractions of the total precipitation when examined on interannual and intraseasonal time scales. Fractional MCC rainfall contributions of 11%–20% were found over much of SSA in all months. MCCs accounted for 20%–30% of the total rainfall between November and February, and 30%–50% in December across northern Argentina and

Paraguay. MCCs also contributed 25%–66% of the total rainfall across smaller areas within the provinces of Mendoza, Neuquén, and La Pampa in west-central Argentina. It is likely that the larger rainfall contributions from MCCs occurred over a region infrequent to MCC activity. This study also shows that the monthly percentage of rainfall resulting from MCCs is much larger in SSA compared to the United States (e.g., 50% versus 20%, respectively).

MCCs account for slightly larger percentages of rainfall when examined by warm season, relative to monthly rainfall contributions. In each warm season, MCCs contributed $\geq 30\%$ of the total rainfall across many areas within SSA, while some areas received $\geq 50\%$. Based on

these findings, MCCs play an essential role in precipitation totals across SSA. However, these results do not necessarily portray the overall impact of MCC rainfall.

This study developed an MCC impact factor (MIF) to determine the effect of MCC rainfall on warm-season precipitation anomalies. The MIF identifies locations where anomaly values changed by ≥0.5 standard deviations in the absence of MCC rainfall, and uses a MIF magnitude ranking scale of 1–6. Results show that the extent and magnitude of the impact of MCC rainfall on precipitation anomalies varies considerably. In some instances, the contribution of MCCs to the total rainfall was relatively low (≤20%) while MIF-1s were collocated with above-average rainfall. In other cases the fractional contribution of MCC rainfall was relatively high (≥30%), which had a high impact on an area (MIF-4s and MIF-5s) and normal rainfall totals surrounded largely by extremely below-average values. Results from the MIF analysis demonstrate that MCC rainfall plays in important role in determining regional anomalous precipitation conditions.

In summary, results from this study extend our global understanding of the role of MCCs in regional precipitation totals. MCCs in SSA are large, long-lived events that produce copious amounts of precipitation over sizeable areas. These events account for large percentages of the total precipitation across SSA, which have been shown to have a substantial impact on regional precipitation anomalies. Furthermore, this study provides a new perspective on monthly and warm-season precipitation patterns across SSA. However, because of the strict MCC classification criteria used in this study, it is likely that the inclusion of other large MCSs would show higher rainfall contributions. Further investigations could examine the differences in fractional contributions of MCC and MCC-like events. These types of studies are becoming increasingly important given that the most recent Assessment Report from the Intergovernmental Panel on Climate Change (Pachauri and Reisinger 2007) states that heavy precipitation events are very likely to increase throughout the next century, contributing to nearly 20% increased rainfall amounts and up to 40% increased annual runoff across portions of SSA. Increases in flood frequency and magnitude from heavy rainfall events will likely contribute to considerable property loss and disruptions of industry, settlement, and society. Last, increases in heavy precipitation events and their resultant flooding will likely lead to an increased risk of injuries, infectious respiratory and skin diseases, and loss of life (Pachauri and Reisinger 2007).

REFERENCES

Anderson, C. J., and R. W. Arritt, 1998: Mesoscale convective complexes and persistent elongated convective systems over the United States during 1992 and 1993. *Mon. Wea. Rev.,* **126,** 578–599.

——, and ——, 2001: Mesoscale convective systems over the United States during the 1997–98 El Niño. *Mon. Wea. Rev.,* **129,** 2443–2457.

Ashley, W. S., T. L. Mote, P. G. Dixon, S. L. Trotter, J. D. Durkee, E. J. Powell, and A. J. Grundstein, 2003: Effects of mesoscale convective complex rainfall on the distribution of precipitation in the United States. *Mon. Wea. Rev.,* **131,** 3003–3017.

Augustine, J. A., and K. W. Howard, 1988: Mesoscale convective complexes over the United States during 1985. *Mon. Wea. Rev.,* **116,** 685–701.

Barber, D., and H. Huhdanpaa, 1996: The quickhull algorithm for convex hulls. *ACM Trans. Math. Software,* **22,** 469–483.

Berbery, E. H., and E. A. Collini, 2000: Springtime and water vapor flux over southeastern South America. *Mon. Wea. Rev.,* **128,** 1328–1346.

——, and V. R. Barros, 2002: The hydrologic cycle of the La Plata Basin in South America. *J. Hydrometeor.,* **3,** 630–645.

Carvalho, L. M. V., C. B. Jones, and B. Liebman, 2002: Extreme precipitation events in southern South America and large-scale convective patterns in the South Atlantic Convergence Zone. *J. Climate,* **15,** 2377–2394.

Curtis, S., 2008: The El Niño–Southern Oscillation and global precipitation. *Geogr. Compass,* **2,** 600–619.

Durkee, J. D., and T. L. Mote, 2009: A climatology of warm-season mesoscale convective complexes in subtropical South America. *Int. J. Climatol.,* doi:10.1002/joc.1961, in press.

Ebert, E., J. E. Janowiak, and C. Kidd, 2007: Comparison of near-real-time precipitation estimates from satellite observations and numerical models. *Bull. Amer. Meteor. Soc.,* **88,** 47–64.

Fritsch, J. M., R. J. Kane, and C. R. Chelius, 1986: The contribution of mesoscale convective weather systems to the warm-season precipitation in the United States. *J. Climate Appl. Meteor.,* **25,** 1333–1345.

Grimm, A. M., S. E. T. Ferraz, and J. Gomes, 1998: Precipitation anomalies in southern Brazil associated with El Niño and La Niña events. *J. Climate,* **11,** 2863–2880.

——, V. R. Barros, and M. E. Doyle, 2000: Climate variability in southern South America associated with El Niño and La Niña events. *J. Climate,* **13,** 35–58.

Huffman, G. J., and D. T. Bolvin, 2007: TRMM and other data precipitation data set documentation. Laboratory for Atmospheres, NASA Goddard Space Flight Center and Science Systems and Applications, 25 pp. [Available online at ftp://meso.gsfc.nasa.gov/pub/trmmdocs/3B42_3B43_doc.pdf.]

——, and Coauthors, 2007: The TRMM Multi-satellite Precipitation Analysis (TMPA): Quasi-global, multiyear, combined-sensor precipitation estimates at fine scales. *J. Hydrometeor.,* **8,** 38–55.

Kummerow, C., and Coauthors, 2000: The status of the Tropical Rainfall Measuring Mission (TRMM) after two years in orbit. *J. Appl. Meteor.,* **39,** 1965–1982.

Laing, A. G., and J. M. Fritsch, 1993: Mesoscale convective complexes in Africa. *Mon. Wea. Rev.,* **121,** 2254–2263.

——, and ——, 2000: The large-scale environments of the global populations of mesoscale convective complexes. *Mon. Wea. Rev.,* **128,** 2756–2776.

——, ——, and A. J. Negri, 1999: Contribution of mesoscale convective complexes to rainfall in Sahelian Africa: Estimates from geostationary infrared and passive microwave data. *J. Appl. Meteor.,* **38,** 957–964.

Lau, K. M., and J. Zhou, 2003: Anomalies of the South American summer monsoon associated with the 1997-99 El Niño-Southern Oscillation. *Int. J. Climatol.,* **23,** 529–539.

Liebmann, B., G. N. Kiladis, C. S. Vera, A. C. Saulo, and L. M. V. Carvalho, 2004: Subseasonal variations of rainfall in South America in the vicinity of the low-level jet east of the Andes and comparison to those in the South Atlantic Convergence Zone. *J. Climate,* **17,** 3829–3842.

Machado, L. A. T., W. B. Rossow, R. L. Guedes, and A. W. Walker, 1998: Life cycle variations of mesoscale convective systems over the Americas. *Mon. Wea. Rev.,* **126,** 1630–1654.

Maddox, R. A., 1980: Mesoscale convective complexes. *Bull. Amer. Meteor. Soc.,* **61,** 1374–1387.

Marengo, J., W. R. Soares, C. Saulo, and M. Nicolini, 2004: Climatology of the low-level jet east of the Andes as derived from the NCEP–NCAR reanalyses: Characteristics and temporal variability. *J. Climate,* **17,** 2261–2280.

McAnelly, R. L., and W. R. Cotton, 1986: Meso-β-scale characteristics of an episode of meso-α-scale convective complexes. *Mon. Wea. Rev.,* **114,** 1740–1770.

——, and ——, 1989: The precipitation life cycle of mesoscale convective complexes over the central United States. *Mon. Wea. Rev.,* **117,** 784–808.

Mechoso, R. C., and Coauthors, 2001: Climatology and hydrology of the La Plata Basin. VAMOS Scientific Study Group on the Plata Basin, 56 pp. [Available online at http://www.clivar.org/organization/vamos/Publications/laplata.pdf.]

Mota, G. V., 2003: Characteristics of rainfall and precipitation features defined by the Tropical Rainfall Measuring Mission over South America. Ph.D. dissertation, University of Utah, 215 pp.

Nesbitt, E., J. Zipser, and D. J. Cecil, 2000: A census of precipitation features in the tropics using TRMM: Radar, ice scattering, and lightning observations. *J. Climate,* **13,** 4087–4106.

Nicolini, M., and A. C. Saulo, 2000: ETA characterization of the 1997–98 warm season Chaco jet cases. Preprints, *Sixth Int. Conf. on Southern Hemisphere Meteorology and Oceanography,* Santiago, Chile, Amer. Meteor. Soc., 330–331.

Nieto Ferreira, R. N., T. M. Rickenbach, D. L. Herdies, and L. M. V. Carvalho, 2003: Variability of South American convective cloud systems and tropospheric circulation during January–March 1998 and 1999. *Mon. Wea. Rev.,* **131,** 961–973.

Orlanski, I., 1975: A rational subdivision of scales for atmospheric processes. *Bull. Amer. Meteor. Soc.,* **56,** 527–530.

Pachauri, R. K., and A. Reisinger, Eds., 2007: *Climate Change 2007: Synthesis Report.* Cambridge University Press, 104 pp.

Ropelewski, C. F., and M. S. Halpert, 1987: Global and regional scale precipitation patterns associated with the El Niño/Southern Oscillation. *Mon. Wea. Rev.,* **115,** 1606–1625.

——, and ——, 1989: Precipitation patterns associated with the high-index phase of the Southern Oscillation. *J. Climate,* **2,** 268–284.

Salio, P., and M. Nicolini, 2007: Mesoscale convective systems over southeastern South America and their relationship with the South American low-level jet. *Mon. Wea. Rev.,* **135,** 1290–1308.

Sapiano, M. R. P., and P. A. Arkin, 2009: An intercomparison and validation of high-resolution satellite precipitation estimates with 3-hourly gauge data. *J. Hydrometeor.,* **10,** 149–166.

Saulo, C., J. Ruiz, and Y. G. Skabar, 2007: Synergism between the low-level jet and organized convection at its exit region. *Mon. Wea. Rev.,* **135,** 1310–1326.

Silva, V. B. S., and T. Ambrizzi, 2006: Inter-El Niño variability and its impact on the South American low-level jet east of the Andes during austral summer—Two case studies. *Adv. Geosci.,* **6,** 283–287.

——, and E. H. Berbery, 2006: Intense rainfall events affecting the La Plata Basin. *J. Hydrometeor.,* **7,** 769–787.

Tollerud, E. I., D. Rodgers, and K. Brown, 1987: Seasonal, diurnal, and geographic variations in the characteristics of heavy-rain-producing mesoscale convective complexes: A synthesis of eight years of MCC summaries. Preprints, *11th Conf. on Weather Modification,* Edmonton, AB, Canada, Amer. Meteor. Soc., 143–146.

Velasco, I., and J. M. Fritsch, 1987: Mesoscale convective complexes in the Americas. *J. Geophys. Res.,* **92,** 9591–9613.

Vera, C., and Coauthors, 2006: The South American Low-Level Jet Experiment. *Bull. Amer. Meteor. Soc.,* **87,** 63–77.

Viana, D. R., 2006: Avaliação da precipitação e desastres naturais associados a complexos convectivos de mesoescala no Rio Grande do Sul entre Outubro e Dezembro de 2003. M.S. thesis, Departamento de Geografia, Universidade Federal do Rio Grande Do Sul, 136 pp.

Zipser, E. J., D. J. Cecil, C. Liu, S. W. Nesbitt, and D. P. Yorty, 2006: Where are the most intense thunderstorms on Earth? *Bull. Amer. Meteor. Soc.,* **87,** 1057–1071.